The line shape and zero-phonon line of the luminescence spectrum from zinc tungstate single crystals

1994 J. Phys.: Condens. Matter 6 5373

(http://iopscience.iop.org/0953-8984/6/28/012)

J. Phys.: Condens. Matter 6 (1994) 5373–5386. Printed in the UK

The line shape and zero-phonon line of the luminescence spectrum from zinc tungstate single crystals

Hong Wang†§, Fernando D Medina†, David D Liu†‖ and Ya-Dong Zhous‡

† Department of Physics, Florida Atlantic University, Boca Raton, FL 33431, USA

‡ Department of Chemical and Environmental Engineering, Beijing Polytechnic University, Beijing, People's Republic of China

Received 1 October 1993, in final form 21 March 1994

Abstract. The blue and infrared (IR) bands of the photoluminescence spectra in the temperature range 11–430 K and excitation bands at 77 and 300 K of zinc tungstate single crystals have been studied. The line shape, obtained from the theory of lattice relaxation and multiphonon transitions, is compared with the experimental results. The temperature dependences of the intensity, the peak position and the line width of the zero-phonon line associated with the IR emission band are investigated experimentally. The results obtained are discussed in terms of the theory of linear and quadratic electron–phonon interactions.

1. Introduction

The luminescence properties of zinc tungstate ($ZnWO_4$) were first reported by Kröger [1]. In recent years, studies concerning the light yield, emission spectrum, afterglow, lifetime and optical properties have been reported [2–5]. They have shown $ZnWO_4$ as a promising new material for x-ray scintillators with luminescence output and afterglow comparable to or better than those of materials currently in use. Another advantage is that the materials used in the preparation of $ZnWO_4$ are non-hygroscopic, non-toxic and cheaper than those used for BGO ($Bi_4Ge_3O_{12}$), a widely used scintillation material.

In order to replace other scintillation materials, however, large single crystals of $ZnWO_4$ of good optical quality are needed. Single crystals of $ZnWO_4$ prepared by the standard Czochralski technique are usually coloured pink. Colour-free crystals can be made by using special annealing techniques or by doping the melt with such metallic elements as niobium or antimony.

Although a blue emission band near 480 nm, for scintillation application, has been previously observed in $ZnWO_4$ [2, 3, 6], and an additional emission band in the near-infrared region (IR emission band) associated with a zero-phonon line (ZPL) and vibrational structure has been reported at low temperature [6–8], a detailed spectroscopic study of the blue and IR emission bands together with the ZPL has not been carried out. In the present study, in addition to the blue emission band from coloured and colour-free samples, the IR emission band of a coloured $ZnWO_4$ sample is studied in the temperature range from 11 to 430 K. Line shapes, obtained from the theory of lattice relaxation and multiphonon transition in

§ Present address: Brookhaven National Laboratory, Building 701, PO Box 5000, Upton, NY 11973, USA.

‖ Present address: Department of Physics, Worcester Polytechnic Institute, Worcester, MA 01609, USA.

0953-8984/94/285373+14$19.50

the linear coupling case, are compared with the experimental results. The temperature dependence of the intensity, the peak position and the line width of the zero-phonon line (ZPL) are investigated experimentally. It is shown that the temperature properties of the ZPL are well described by the theory of electron–phonon interactions if one takes into account the quadratic coupling between electrons and acoustic phonons.

2. Experimental details

Single crystals of $ZnWO_4$ were grown in air by a balance-controlled Czochralski technique. $ZnWO_4$, in which WO_6 octahedra exist as luminescence centres [9, 10], has the monoclinic Wolframite structure with C_{2h} point group symmetry and $P2/c$ space group symmetry with two formula units per unit cell [11]. These samples were checked by x-ray diffraction (Cu Kα line) and were all found to be single phased.

The samples used in this work were optically transparent in the range from 0.3 to 5.0 μm. They were mounted on a sample holder (high-thermal-conductivity copper) attached to the cold finger of a closed-cycle helium refrigerator capable of controlling temperature within ± 0.1 K in the range 11–430 K. The blue emission bands of coloured and colour-free samples were obtained using a high-pressure mercury lamp, a VIS cut-off filter and a Spex 1403 double grating spectrometer with a cooled photomultiplier tube (PMT). Measurement of the temperature dependence of the ZPL with higher resolution was obtained, using a Spex 1403 double-grating spectrometer with an interference filter, by a cooled PMT. In the experimental investigation of the ZPL, various excitation frequencies (476.5, 488.0, 496.5, 510.7 and 514.5 nm) were used. The IR emission band was obtained using the 514.5 nm line of an argon-ion laser, two UV–VIS cut-off filters, a Spex 1870 spectrometer with an IR detector, a lock-in amplifier and a boxcar integrator. The spectra were recorded in the region 750–1300 nm, and calibrated using a standard quartz tungsten halogen (QTH) lamp. Excitation spectra were recorded on a Perkin–Elmer LS 50 luminescence spectrometer at 300 and 77 K.

3. Results and discussion

3.1. Temperature dependence of the emission bands

The temperature dependences of the blue emission band from coloured and colour-free samples, and the IR emission band from the coloured sample, have been studied. The spectra were obtained at 10 K intervals in the temperature region from 11 to 430 K. A typical experimental result for the blue emission band from a coloured sample is shown in figure 1.

There are three primary effects for all three emission bands. Firstly, the total integrated intensities decrease gradually with increasing temperature: at high temperature, for example, $T = 400$ K, the integrated intensities are reduced to about 1% of the maximum integrated intensities. The measurements of the temperature dependence of the integrated intensities give a quenching temperature T_q, defined as the temperature where the integrated intensity is half of the maximum, near 340 K for the blue emission bands of both coloured and colour-free samples, and near 245 K for the IR emission band of the coloured sample.

Secondly, the peak positions of all bands show almost no change for $T < 100$ K. For higher temperatures, the peak positions are all shifted to higher energies with increasing

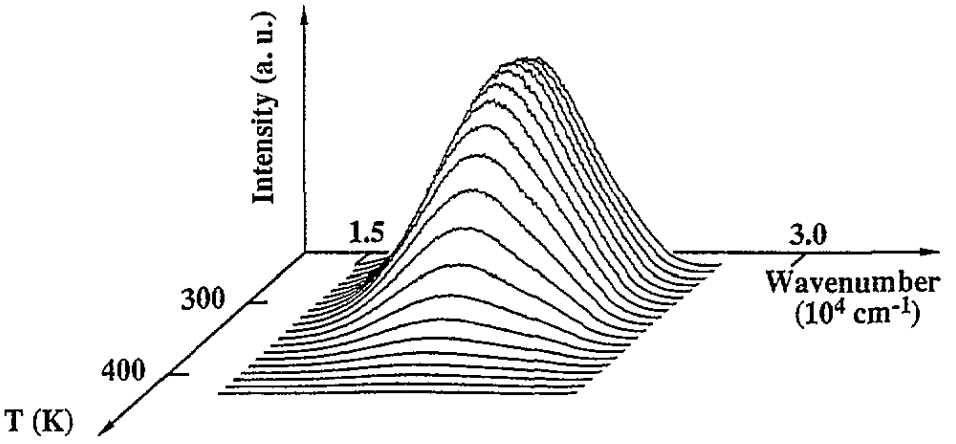

Figure 1. The blue emission band of coloured $ZnWO_4$ as a function of temperature.

temperature. A shift of a broad band to lower energy with increasing temperature is expected as a consequence of thermal expansion [12]. However, the anomalous shift to higher energy may be explained in terms of non-radiative transitions, which do not occur with significant probability at low temperature.

Thirdly, the full width at half maximum (FWHM) $\Gamma(T)$ of all bands shows almost no change for $T < 100$ K, but with increasing temperature the emission bands broaden for $T > 100$ K. For example, for the blue emission spectra of the coloured sample, $\Gamma(100\ \text{K}) \simeq 4300\ \text{cm}^{-1}$, whereas $\Gamma(400\ \text{K}) \simeq 5800\ \text{cm}^{-1}$. This temperature dependence of FWHM is not weak. It is due to multiphonon transitions, in which electrons excited into an electronic excited state relax non-radiatively to the vibrational ground state of that particular electronic state by emission of phonons. The effect of non-radiative transitions to the ground state are negligible in the low-temperature region. As temperature increases, the electrons in the lowest excited state will be thermally excited to higher vibrational states of that electronic state. In the single-configurational-coordinate (SCC) model, it is obvious that increasing temperature broadens the emission band.

Earlier measurements on $CaWO_4$ [13, 14], $PbWO_4$ [15, 16], $SrWO_4$ [17], $BaWO_4$ [17], $CdWO_4$ [18] and $MgWO_4$ [19], showing similar results, indicate that the blue emission is the intrinsic tungstate emission. This optical transition involved in the luminescence of W (d^0)–O(−II) groups might be due to charge-transfer transition between the O 2p orbitals and the empty d orbitals of the central W ion [20, 21]. On the other hand, the IR emission band is suggested to result from defected W–O groups [6].

In the linear-coupling case using the SCC model, the experimental data on the temperature dependence of the emission spectra allows the determination of the important parameters such as the Huang–Rhys parameter S, which characterizes electron–phonon interactions [22], and the average phonon energy $\overline{\hbar\omega}$. These are given by [23–25]

$$[\Gamma(T)]^2 \simeq [8 \ln 2 S(\overline{\hbar\omega})^2] \coth\left(\frac{\overline{\hbar\omega}}{2k_B T}\right). \tag{1}$$

The values of the parameters obtained with a least-squares method are summarized in table 1.

Table 1. Parameters of the SCC model in the linear-coupling case.

	$ZnWO_4$ (coloured)		$ZnWO_4$ (colour-free)
	blue	IR	blue
S (±0.1)	30.3	4.6	23.6
$\overline{\hbar\omega}$ (cm^{-1}) (±2.0)	329.8	244.6	369.2

Some significant results are found in table 1. Notice that the Huang–Rhys parameters S for the blue emission band of coloured and colour-free samples are both much larger than six, which corresponds to a strong coupling between electrons and phonons. On the other hand, for the IR emission band of the coloured sample, S is nearly 4.6, which corresponds to an intermediate-coupling case [23]. In fact, the blue emission bands of two different samples are bell shaped without fine vibrational structure, even at temperatures down to 11 K, whereas the ZPL associated with the fine vibrational structure of the IR emission band of the coloured sample is observable at $T \leqslant 60$ K. This is in good agreement with luminescence theory.

It is interesting to compare the blue emission and corresponding excitation bands of two different samples. The band position, bandwidth and band shape are nearly the same for the blue emission bands from two different samples at low temperature, whereas for the excitation bands, the 'excitation edge' (which is defined as the position where the intensity is half of the maximum) of the coloured sample is shifted about 5 nm to higher energies relative to the colour-free sample. This is shown in figure 2, in which the excitation spectra of bleached samples of $ZnWO_4$:Nb and $ZnWO_4$:Sb are also shown. This may be attributed to self-absorption, since there is a broad absorption band near 500 nm for the coloured sample [5]. A detailed discussion will be presented elsewhere.

3.2. Line shape of the emission bands

In the framework of linear electron–phonon coupling, an expression for the emission band shape at temperature T is derived by carrying out the Frank–Condon approximation and the thermal average over the initial vibrational states. It can be shown that the emission line shape as a function of temperature is given by [24–27]

$$W_p = A^2[(n+1)/n]^{p/2}e^{-S(2n+1)}I_p\left(2S\sqrt{n(n+1)}\right) \tag{2}$$

where n is the average occupation number of the vibrational mode, p expresses the net number of phonons created in the electronic transition, $I_p(x)$ is the modified Bessel function, A^2 is the transition electronic factor and W_p in equation (2) is also called the HRP (Huang–Rhys–Pekar) function. The emission band shape now is expressed as a function of temperature T and the Huang–Rhys factor S, and thus the spectroscopic features of the broad emission band such as the temperature dependence of the integrated intensity can be described by using the line shape function.

The fit of the experimental line shape of the emission band to equation (2), which is predicted by the SCC model with linear coupling using the model parameters in table 1, is shown in figure 3 for the blue emission band of the coloured sample and in figure 4 for the IR emission band of the coloured sample. As can be seen the fits for the blue emission bands are acceptable. This indicates that the dominant electron–phonon coupling term of the blue emission is linear.

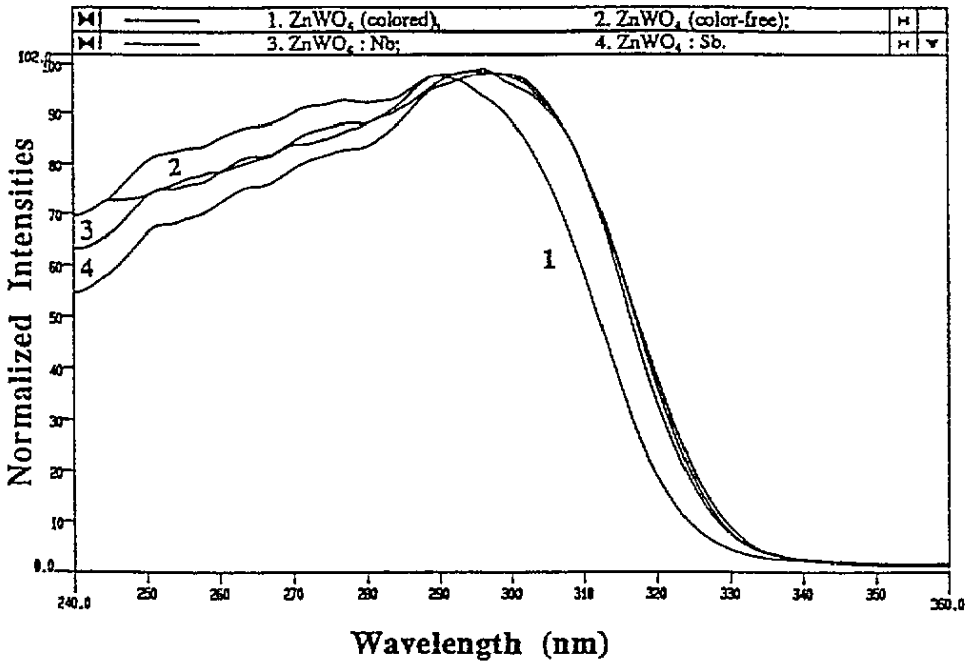

Figure 2. Excitation spectra of coloured $ZnWO_4$, colour-free $ZnWO_4$, $ZnWO_4$:Nb and $ZnWO_4$:Sb ($E_{em} = 460$ nm, $T = 300$ K).

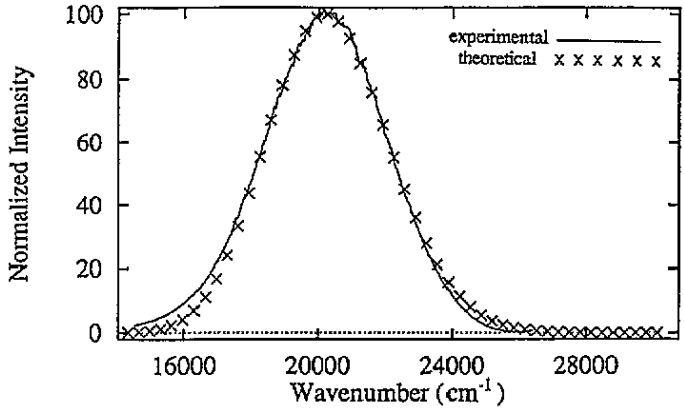

Figure 3. The band shape of the blue emission from coloured $ZnWO_4$ at 11 K.

It is noticed that the theoretical line cannot fit the experimental line well for the IR emission band of the coloured sample. The line shape function in equation (2) is mainly based on only two approximations: the linear-coupling limit and the single-phonon-frequency model. For the emission band corresponding to a strong-coupling case, if the ratio of transition energy $\bar{E}$ to the average phonon energy $\overline{\hbar\omega}$ is less than about 70, the

single-frequency model is a reasonably good approximation to the multi-frequency model, which is the real case [28]. For the blue bands of coloured and colour-free samples and the IR emission band, the ratios are all less than 70. Thus one is able to simply apply the single-phonon-frequency model. The reason that the fit is not good for the IR band may be the existence of considerable non-linear coupling between electrons and phonons.

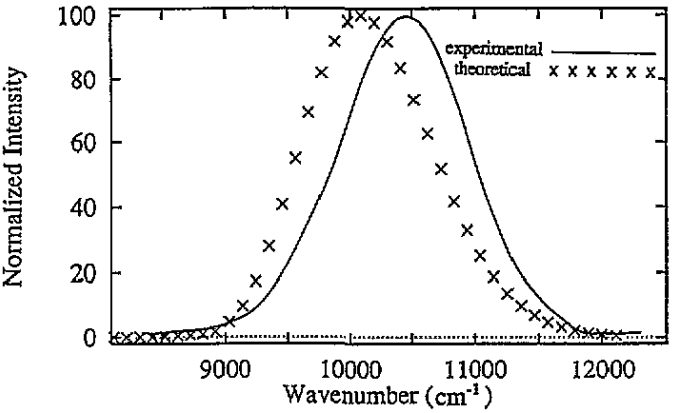

Figure 4. The band shape of the IR emission from coloured $ZnWO_4$ at 11 K.

3.3. Temperature dependence of the integrated intensity of the zero-phonon line

The experimental study of the temperature dependence of the ZPL provides very useful information on the linear and non-linear electron–phonon interactions. The temperature dependence of the ZPL associated with an infrared emission band was observed from a coloured $ZnWO_4$ sample. The results (figure 5) show that as temperature increases, the integrated intensity of the ZPL decreases, the peak position shifts to lower energies (red shift) and the line width broadens. For temperatures above 60 K, the ZPL cannot be observed, which may be attributed to thermal quenching. The experimental results also show that the peak position of the ZPL is independent of the excitation energies in the wavelength range of 457.9–514.5 nm.

Equation (2) describes the line shape at temperature T. At $T = 0$ K and $p = 0$, phonons are not involved in the transition, i.e. it is a purely electronic transition, or zero-phonon transition, and only the $n = 0$ vibrational state is occupied; thus the ZPL has the intensity

$$W_{p=0}(T = 0, E) \propto e^{-S}\delta(E_{ji} - E) \tag{3}$$

where E_{ji} is the energy of the transition between the zero vibrational levels of initial and final states, i.e., the energy of the zero-phonon transition.

In addition to ZPL-type transitions, there is also a finite probability that, in the final state, not only the vibronic modes of the impurity atom or molecule, but also those of the host system, become excited. Transitions that correspond to a change in phonon state of the lattice ($p \neq 0$) are called multi-phonon transitions. Multi-phonon transitions, in which

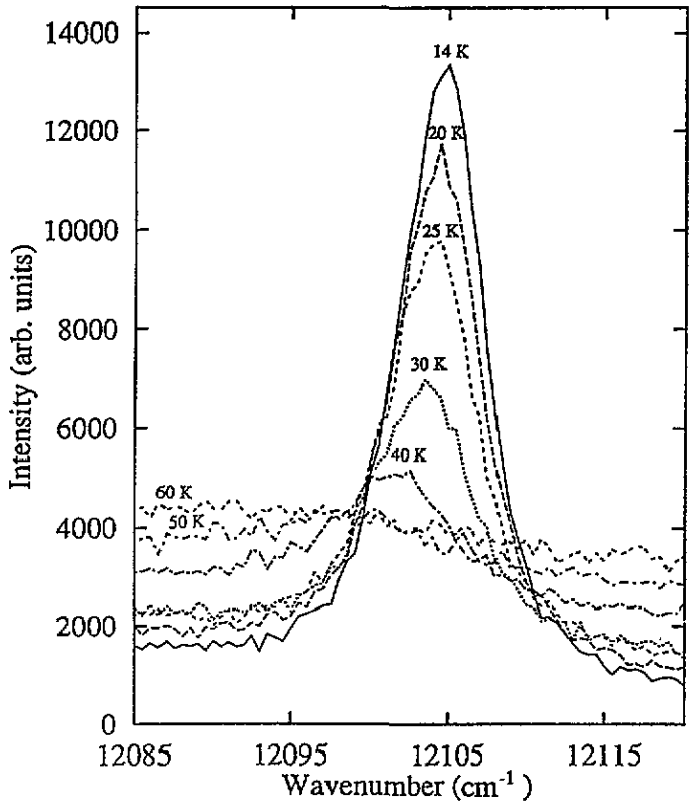

Figure 5. The temperature dependence of the ZPL of coloured $ZnWO_4$ from 14 to 60 K.

n phonons participate, will lead to the appearance of a broad phonon sideband accompanying the ZPL. At low temperature, the basic feature on the ZPL and the phonon sideband can also be interpreted by the value of the Huang–Rhys parameter S [29]

$$I_{ZP}/(I_{ZP} + I_{band}) \simeq e^{-S} \tag{4}$$

where I represents the integrated intensity.

At $T > 0$, the zero-order Bessel function is approximately unity if the temperature is not very high. Thus equation (2) can be simplified as [24]

$$W_{p=0}(T) \propto \exp\left[-S \coth\left(\frac{\overline{\hbar\omega}}{2k_B T}\right)\right] = \exp[-S(2n+1)]. \tag{5}$$

On the other hand, the basic feature on the ZPL and the phonon sideband can also be explained by using the Debye approximation at finite temperature [29]

$$\frac{I_{ZP}}{I_{ZP} + I_{band}} = \exp\left\{-S\left[1 + 4\left(\frac{T}{T_D}\right)^2 \int_0^{T_D/T} dx \, \frac{x}{e^x - 1}\right]\right\}$$
$$\simeq \exp\left\{-S\left[1 + \left(\frac{2\pi^2}{3}\right)\left(\frac{T}{T_D}\right)^2\right]\right\} \qquad \text{if } T \ll T_D \tag{6}$$

Table 2. The Huang–Rhys parameter S and the Debye temperature T_D of the IR emission in $ZnWO_4$.

S			
$\exp[-S(2n(\bar{\omega})+1)]$	$\exp\{-S[1+6.6(T/T_D)^2]\}$	$[\Gamma(0)/(2.36\overline{\hbar\omega})]^2$	T_D (K)
3.5	4.3	4.6	173

where T_D is defined as the Debye temperature.

It can be seen that in the low-temperature limit, equation (6) becomes the same as equation (4). It follows from the above expressions that when the temperature is increased, the integrated intensity of the ZPL has to decrease. It is obvious that the measurement of the integrated intensity distribution as a function of temperature enables one to determine the Huang–Rhys parameter S and the Debye temperature T_D.

According to equation (4), which is predicted by theory in the linear-coupling approximation, the Huang–Rhys parameter S is simply related to the integrated intensity of the ZPL at 0 K. This equation cannot be used accurately since the lowest temperature used in this investigation is 11 K. However, as seen in figure 5, the ZPL can be observed when $T \leqslant 60$ K, which allows one to use equations (5) and (6) to discuss the temperature dependence of the integrated intensity of the ZPL, if T_D is much higher than 60 K. The results fitted by using the least-squares method are shown in table 2. The third value of S in table 2 is based on the SCC model using equation (1). The agreement among the values of S is very satisfactory. The value of 3.5 obtained by fitting equation (5) to the data is a little small, which may result from the simplification of the Bessel function being unity at low temperature. The Debye temperature of coloured $ZnWO_4$ fitted by using equation (6) is also listed in table 2.

3.4. Temperature shift and broadening of the zero-phonon line

In the linear coupling approximation, the ZPL is a δ function with position and 'line width' that do not depend on temperature [23]. However, this is not always the case. For systems having both linear and considerable quadratic interaction terms, their behaviour of the ZPL, which has a certain peak position, a finite line width and asymmetric line shape, is temperature dependent, as observed in $ZnWO_4$. Thus one needs to consider the quadratic contribution to electron–phonon coupling.

In general, the potential energy curves of the ground and excited states are different. The difference in potential energy results from additional terms, i.e., quadratic terms, in the electron–phonon coupling that determine the nature and shape of each vibronic band. Skinner and Hsu [30] have discussed the broadening and spectral shift effects of the ZPL in a non-perturbative theory. Using the Debye model, as temperature increases the interactions between electrons and acoustic phonons result in a line shift $\delta\nu$ and a line width broadening $\Delta\nu$, given by

$$\delta\nu = \omega_D \frac{3}{4\pi} \frac{W}{1+W} \left(\frac{T}{T_D}\right)^4 \int_0^{T_D/T} dx \, \frac{x^3}{e^x - 1} \tag{7}$$

and

$$\Delta\nu = \omega_D \frac{9}{4} \left(\frac{W}{1+W}\right)^2 \left(\frac{T}{T_D}\right)^7 \int_0^{T_D/T} dx \, \frac{x^6 e^x}{(e^x - 1)^2} \tag{8}$$

where $\hbar\omega_D = k_B T_D$, W is the quadratic coupling constant and $W > -1$. For $T \ll T_D$, these quantities display T^4 and T^7 temperature dependences, respectively. For $T \gg T_D$, they depend on T and T^2, respectively. It is interesting to notice that in the weak-coupling limit, i.e., $|W| \ll 1$, one obtains the familiar weak-coupling results [31].

It has been shown that an increase in temperature causes both blue and red shifts, depending on the material [32]. The magnitudes of the shifts for different crystals differ considerably. Since the zero-phonon transition energy, in the general case, can be considered as a thermodynamic quantity, a function of the crystal temperature T and its volume V, the shift of the ZPL with temperature at constant pressure P can be written in the form

$$(dE/dT)_P = (\partial E/\partial T)_V + (\partial E/\partial V)_T(\partial V/\partial T)_P. \tag{9}$$

Hence, the ZPL shift is equal to the sum of two shifts: the term $(\partial E/\partial T)_V$ is determined by the temperature change of the electron–phonon interaction at constant volume, and depends on the presence of terms linear and quadratic in the nuclear coordinates, while the term $(\partial E/\partial V)_T(\partial V/\partial T)_P$ is related to the thermal expansion of the lattice due to the anharmonicity of the crystal vibrations.

The sign and magnitude of the temperature shift of the ZPL depend on the relation between the shift due to thermal expansion of the crystal lattice and the shift due to electron–phonon interactions at constant volume. Sapozhnikov [32], summarizing his work, pointed out that for all systems studied, the shift of the ZPL due to thermal expansion of the lattice occurs to the blue, while the shift caused by electron–phonon interactions occurs to the red with increasing temperature and its absolute value is smaller than the former. The temperature shift of the ZPL in the IR emission spectra of coloured $ZnWO_4$ has been experimentally measured. Our experimental results, as can be seen from figure 5, show that as temperature increases, the ZPL shows a red shift, similar to that of the F centres in CaO [33]. In addition, in our previous Raman spectroscopic study on $ZnWO_4$ [34], we found that at low temperatures, i.e., $T < 60$ K, the frequencies and the line widths of the modes do not change. This indicates that thermal expansion can be reasonably neglected. In other words, at low temperature, the sample can be regarded as a very 'hard' crystal. In this case, the shift associated with the electron–phonon interaction is the dominant contribution and the second term in equation (9) can be neglected. Thus the shift due to electron–phonon coupling considerably exceeds the shift caused by the thermal expansion of a crystal and, therefore, determines the whole experimentally observed line shift. In fact, linear electron–phonon coupling alone does not produce a shift of the ZPL [35], and there are no contributions from the interactions between electrons and optical phonons to the shift of the ZPL [30]. In addition, the contribution to the shift from localized modes may be ignored, as indicated by the fact that the peak position of the ZPL is independent of excitation energy [36]. Therefore, it turns out that the main contributions to the shift of the ZPL originate from quadratic interactions between electrons and acoustic phonons. Hence one can use the theoretical expression equation (7) to discuss electron–phonon interactions. In figure 6, the experimental and theoretical line shifts with temperature, expressed by crosses and a solid curve, respectively, are given. Fitting the data, using the least-squares method, resulted in a quadratic electron–phonon coupling constant $W \simeq -0.25 \pm 0.01$ and a Debye temperature $T_D \simeq 198 \pm 15$ K.

As can be seen from figure 5, in addition to a line shift as temperature increases, line width broadening has been experimentally obtained. Linear electron–phonon interactions alone do not produce line broadening, neither does the coupling to the optical phonons [35], and thermal expansion does not contribute to line width [37]. In addition, the phonon–phonon interactions are, in general, weaker than the electron–phonon coupling for optical

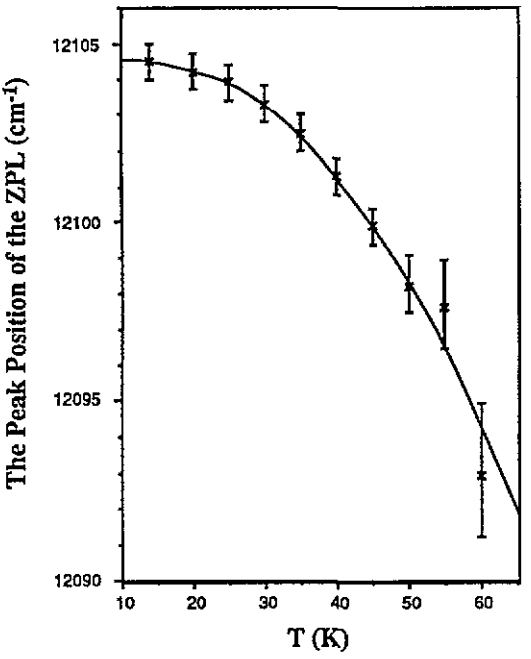

Figure 6. The temperature dependence of the peak position of the ZPL from coloured $ZnWO_4$.

transitions [38]. Thus the observed line width broadening of the ZPL should be mainly attributed to the quadratic coupling between electrons and acoustic phonons.

The shape of the ZPL is determined by the mechanism of its broadening. For example, the radiative decay and also the direct and Raman processes give a Lorentzian line shape [31]. On the other hand, the shape of the non-uniformly broadened line in many cases may be Gaussian, for example, for the interaction with point defects randomly distributed in the crystal [32]. As temperature increases, in general, the ZPL broadening results from different mechanisms, some of which predict Gaussian, while others Lorentzian line shapes. The shape of the ZPL in a real crystal at finite temperature should be considered as a convolution of Gaussian and Lorentzian distributions, i.e., should be described by a Voigt function [32]. Technically, one needs to consider the instrumental factors, which introduce some distortion to the shape of the ZPL. The raw data acquired in this experiment is the convolution of the term of the ZPL with the slit function of the spectrometer, which is usually regarded as a Gaussian and was found to have a 3.7 cm^{-1} line width (FWHM). Thus the spectral line width data had to be corrected.

In order to quantitatively compare the experimental temperature dependence of the line width with the theory of electron–phonon interactions, one needs to separate the Lorentzian and Gaussian components of the observed line. This has been done with the aid of the numerical tables of Posener [39] and computer deconvolution techniques. The background of the ZPL contributed by multi-phonon transitions has been subtracted by numerical methods using a computer. Notice that there are three independent components, which are the Lorentzian component Γ_L^{true} of the ZPL, the Gaussian component Γ_G^{true} of the ZPL and the term $\Gamma_G^{instrum}$, the instrumental contribution. These three independent components are convoluted together. In order to eradicate the instrumental contribution, the deconvolution was made

in the following steps. First, we have deconvoluted the experimental line widths of the ZPL into two components: a Gaussian component Γ_G^{exp}, and a Lorentzian component Γ_L^{true}. Next, the terms of Γ_G^{true} have been obtained, considering that Γ_G^{exp} is the convolution of Γ_G^{true} and $\Gamma_G^{instrum}$. Now, we have taken out the instrumental component, and obtained two independent components Γ_L^{true} and Γ_G^{true} of the ZPL. Finally, the line widths Γ_L^{cov} and Γ_G^{cov} have been convoluted assuming a convolution of either two Gaussians or two Lorentzians of those two independent components of the ZPL. The true line widths should have values between those extremes; the average values, $\Gamma_{average}^{cov}$ will be considered in the following discussion. The results are given in table 3.

Table 3. Line widths of the ZPL in cm^{-1} at various temperatures.

T	Deconvolution from experimental results			ξ	Convoluted Γ_L^{true} and Γ_G^{true} of observed (fitted by using equation (8))		
(K)	Γ_L^{true}	Γ_G^{exp}	Γ_G^{true}	$(\Gamma_L^{true}/\Gamma_G^{true})$	Γ_L^{cov}	Γ_G^{cov}	$\Gamma_{average}^{cov}$
14	3.4	4.4	2.4	1.4	5.7 (5.4)	4.1 (3.9)	4.9 (4.7)
20	3.6	4.4	2.4	1.5	6.0 (5.7)	4.3 (4.1)	5.2 (4.9)
25	3.8	4.5	2.5	1.5	6.3 (6.4)	4.5 (4.6)	5.4 (5.5)
30	3.9	6.0	4.7	0.83	8.6 (7.9)	6.1 (5.7)	7.4 (6.8)
35	4.1	6.5	5.3	0.77	9.4 (10.5)	6.7 (7.5)	8.1 (9.0)
40	4.7	8.1	7.2	0.65	11.9 (14.1)	8.7 (10.1)	10.3 (12.1)
45	8.0	12.5	12.0	0.67	20.0 (18.8)	14.4 (13.6)	17.2 (16.2)
50	9.5	16.9	16.5	0.58	26.0 (24.7)	19.0 (18.0)	22.5 (21.3)
55	11.5	20.9	20.5	0.56	32.0 (31.6)	23.5 (23.2)	27.8 (27.4)
60	13.0	25.7	25.5	0.51	38.5 (39.6)	28.6 (29.2)	33.5 (34.4)

Several interesting results can be deduced from table 3. Firstly, the observed line widths of the ZPL at the lowest temperature are in the range of a few cm^{-1}, corresponding to the inhomogeneous broadening predicted by luminescence theory. As temperature increases the line widths are broadened predominantly by the interactions between electrons and acoustic phonons, while thermal expansion effects can be ignored. Secondly, at lower temperature, the Lorentzian component becomes larger than the Gaussian. At $T < 25$ K, the line widths show little thermal broadening. Due to radiative decay, the ZPL has a finite width and its true shape is described by a Lorentizian curve at low temperature. In addition, Raman and direct processes also have contributions to the Lorentzian line shape. Since the line width caused by radiative decay is very narrow, and the probability of direct processes is small at low temperature, it is reasonable to assume that the contribution from the Raman process is the main part of the Lorentzian component of the ZPL at low temperature, which is similar to the case of R lines in ruby [31]. Crystal defects such as dislocations and point defects, for example, colour centres that are randomly distributed in a crystal, affect the electronic transition. The value of the temperature-independent non-uniform 'residual' broadening, Γ_0, is of the order of several cm^{-1}. As a result, it causes a Gaussian broadening in the shape of the ZPL even at low temperature. In the interaction between electronic transitions and these crystal defects and the Raman process that causes Gaussian and Lorentzian line shapes, respectively, resulting in the residual line width of the ZPL. Finally, it is found that the ratio ξ of Γ_L^{true} to Γ_G^{true} remains almost the same when $T < 25$ K. However, above 25 K, the value of ξ decreases as temperature increases, which is contrary to the observation by

Sapozhnikov [32]. This experimental result indicates that the interaction between electronic transitions and phonons associated with defects becomes stronger, and the Raman and direct processes may not play the leading roles as temperature increases.

The temperature broadening of the ZPL associated with the IR emission band from coloured $ZnWO_4$ is well described by equation (8). The fitted values of the line widths at the different temperatures are listed in table 3. The quadratic coupling constant W, the Debye temperature T_D and the residual line width $\Gamma_0^{residual}$ of the ZPL were fitted by using the least-squares method and are listed in table 4. For comparison, the fitted values of W and T_D obtained from the line shift discussion, and T_D obtained from analysis of the temperature dependence of the intensity, are also listed in this table.

Table 4. The quadratic coupling constant W, the Debye temperature T_D (K), and the residual line width $\Gamma_0^{residual}$ (cm^{-1}) of the ZPL.

	Convolution method	W (± 0.01)	T_D (± 10)	$\Gamma_0^{residual}$ (± 0.2)
By line width broadening	Extreme assuming two Lorentzians	−0.33	185	5.4
	Extreme assuming two Gaussians	−0.30	192	3.9
	The average of two extremes	−0.32	188	4.6
By line shift observation	—	−0.25	198	—
By analysis of intensity	—	—	173	—

In table 4, it can be seen that the parameters were fitted reasonably well; the values of W and T_D assuming the true line width is the average of two extreme cases are just between those assuming the extreme cases, i.e., convoluted assuming two Lorentzians and two Gaussians, respectively. In addition, considering the values of W and T_D obtained in the analyses of line shift and intensity, the quadratic coupling constant W is near -0.29 ± 0.05 and the Debye temperature is 185 ± 25 K. Since $|W|$ is 0.29, not much smaller than unity, the quadratic electron–phonon interaction is in fact not attributed to weak coupling [30]; it suggests that this interaction is within the intermediate-quadratic-coupling case.

Durville *et al* [40] and Ragan *et al* [41] pointed out that the Debye temperature T_D obtained in this work is not necessarily the same as the one that determines the heat capacity, since not all phonons are coupled to the electronic transition. The heat capacity of $ZnWO_4$ was reported by Lyon and Westrum [42]; however, they did not give the Debye temperature. Birang and Bartolo [43] found that different Debye temperatures may be used in explaining line shift and line width broadening as temperature increases. Then, it simply indicates that different effective phonon distributions are active in the processes contributing to the temperature dependence of line shift and line width broadening. However, it is noticed that Skinner and Hsu [30] insisted that the Debye temperature T_D should be the same in the determination of the specific heat and that of optical dephasing (line width broadening) experiments.

4. Conclusion

In the linear-coupling case, the line shapes of the blue emission bands of coloured and

colour-free $ZnWO_4$ crystals are well explained by using the SCC model. The electron–phonon interactions of the blue bands can be considered as the strong-coupling case, whereas, since the value of Huang–Rhys parameter S of the IR emission band is nearly 4.6, the electron–phonon interactions correspond to the intermediate case.

From the temperature dependence of the ZPL it can be concluded that (i) because of interactions between electrons and acoustic phonons, the position of the ZPL shifts to lower energies (red shift) and the line width broadens as temperature increases, and (ii) an analysis of the temperature dependence of the integrated intensity, red shift and line width broadening of the ZPL yields a quadratic coupling constant $W = -0.29 \pm 0.05$ and a Debye temperature $T_D = 185 \pm 25$ K.

References

[1] Kröger F A 1948 *Some Aspects of the Luminescence of Solids* (Amsterdam: Elsevier)
[2] Oi T, Takagi K and Fukazawa T 1980 *Appl. Phys. Lett.* **36** 278
[3] Grabmaier B C 1984 *IEEE Trans. Nucl. Sci.* **NS-31** 372
[4] Zhu Y C, Lu J G, Shao Y Y, Sun H S, Li J, Wang S Y, Dong B Z, Zheng Z P and Zhou Y D 1986 *Nucl. Instrum. Methods Phys. Res.* A **244** 579
[5] Wang H, Liu Y, Zhou Y D, Chen G, Zhou T, Wang J H and Hu B Q 1989 *Acta Phys. Sin.* **38** 670
[6] Wang H, Medina F D and Zhou Y D 1993 *Chem. Phys. Lett.* **205** 497
[7] Wang H, Medina F D and Zhou Y D 1990 *Opt. Photo. News* **1** A125
[8] Yamaga M, Marshall A, O'Donnell K P and Henderson B 1990 *J. Lumin.* **47** 65
[9] Wang H, Liu Y, Zhou Y D, Chen G, Hu B Q and Gu B Y 1988 *Acta Phys. Sin.* **37** 43
[10] Liu Y, Wang H, Chen G, Zhou Y D, Gu B Y and Hu B Q 1988 *J. Appl. Phys.* **64** 4651
[11] Filipenko O S, Pobodimskaya E A and Belov N V 1968 *Sov. Phys.–Crystallogr.* **13** 127
[12] Henderson B, Yamaga M, Gao Y and O'Donnell K P 1992 *Phys. Rev.* B **46** 652
[13] Treadaway M J and Powell R C 1974 *J. Chem. Phys.* **61** 4003
[14] Grasser R and Scharmann A 1976 *J. Lumin.* **12** 473
[15] van Loo W 1975 *Phys. Status Solidi* a **27** 565
[16] Groenink J A and Blasse G 1980 *J. Solid State Chem.* **32** 9
[17] Blasse G and Schipper W J 1974 *Phys. Status Solidi* **25** K163
[18] Lammers M J J, Blasse G and Robertson D S 1981 *Phys. Status Solidi* a **63** 569
[19] Tews W, Herzog G and Roth I 1985 *Z. Phys. Chem.* **266** 989
[20] van Oosterhaut A B 1977 *Phys. Status Solidi* a **41** 607
[21] Blasse G 1990 *Chem. Phys. Lett.* **175** 237
[22] Huang K and Rhys A 1950 *Proc. R. Soc.* A **204** 406
[23] Hayes W and Stoneham A M 1985 *Defects and Defect Processes in Nonmetallic Solids* (New York: Wiley)
[24] Henderson B and Imbusch G F 1989 *Optical Spectroscopy of Inorganic Solids* (Oxford: Clarendon)
[25] Struck C W and Fonger W H 1991 *Understanding Luminescence Spectra and Efficiency Using W_p and Related Functions* (Berlin: Springer)
[26] Huang K 1981 *Prog. Phys.* **1** 31
[27] Illarramendi M A, Fernández J, Balda R, Lucas J and Adam J L 1991 *J. Lumin.* **47** 207
[28] Huang K and Gu Z Q 1983 *Physica* **117 & 118** 552
[29] Fitchen D B, Silbee R H, Fulton T A and Wolf E L 1963 *Phys. Rev. Lett.* **11** 275
[30] Skinner J L and Hsu D 1986 *Adv. Chem. Phys.* **65** 1
[31] McCumber D E and Sturge M D 1963 *J. Appl. Phys.* **34** 1682
[32] Sapozhnikov M N 1976 *Phys. Status Solidi* b **75** 11
[33] Glasbeek M, Smith D D, Perry J W, Lambert W R and Zewail A H 1983 *J. Chem. Phys.* **79** 2145
[34] Wang H, Medina F D, Zhou Y D and Zhang Q N 1992 *Phys. Rev.* B **45** 10356
[35] Hsu D and Skinner J L 1984 *J. Chem. Phys.* **81** 1604
[36] Rabane L A 1972 *Proc. Int. Seminar on Physics of Impurities Centers in Crystals (Tallinn, 1970)* ed G S Zavt (Tallinn: Academy of Sciences of the Estonian SSR) p 353
[37] Jenkins T E 1986 *J. Phys. C: Solid State Phys.* **19** 1065
[38] Skinner J L 1988 *Ann. Rev. Phys. Chem.* **39** 463

[39] Posener D W 1959 *Aust. J. Phys.* **12** 184
[40] Durville F, Dixon G S and Powell R 1987 *J. Lumin.* **36** 221
[41] Ragan D D, Gustavsen R and Schiferl D 1992 *J. Appl. Phys.* **72** 5539
[42] Lyon W G and Westrum E F Jr 1974 *J. Chem. Thermodyn.* **6** 763
[43] Birang B and Barolo B D 1967 *Phys. Rev.* **38** 5133